Cones perform a non-linear transformation on natural stimuli

D. Endeman[1] and M. Kamermans[1,2]

[1] *Netherlands Institute for Neuroscience, Meibergdreef 47, 1105 BA Amsterdam, The Netherlands*
[2] *Department for Neurogenetics, Academic Medical Center, University of Amsterdam, Meibergdreef 15, 1105 AZ Amsterdam, The Netherlands*

Visual information in natural scenes is distributed over a broad range of intensities and contrasts. This distribution has to be compressed in the retina to match the dynamic range of retinal neurons. In this study we examined how cones perform this compression and investigated which physiological processes contribute to this operation. M- and L-cones of the goldfish were stimulated with a natural time series of intensities (NTSI) and their responses were recorded. The NTSI displays an intensity distribution which is skewed towards the lower intensities and has a long tail into the high intensity region. Cones transform this skewed distribution into a more symmetrical one. The voltage responses of the goldfish cones were compared to those of a linear filter and a non-linear biophysical model of the photoreceptor. The results show that the linear filter under-represents contrasts at low intensities compared to the actual cone whereas the non-linear biophysical model performs well over the whole intensity range used. Quantitative analysis of the two approaches indicates that the non-linear biophysical model can capture 91 ± 5% of the coherence rate (a biased measure of information rate) of the actual cone, where the linear filter only reaches 48 ± 8%. These results demonstrate that cone photoreceptors transform an NTSI in a non-linear fashion. The comparison between current clamp and voltage clamp recordings and analysis of the behaviour of the biophysical model indicates that both the calcium feedback loop in the outer segment and the hydrolysis of cGMP are the major components that introduce the specific non-linear response properties found in the goldfish cones.

(Received 21 July 2009; accepted after revision 11 December 2009; first published online 14 December 2009)
Corresponding author M. Kamermans: Netherlands Institute for Neuroscience, Department of Retinal Signal Processing, Meibergdreef 47, 1105 BA Amsterdam, The Netherlands. Email: m.kamermans@nin.knaw.nl

Abbreviations ERG, electroretiongram; PDE, phosphodiesterase; pdf, probability density function; SNR, signal-to-noise ratio; NTSI, natural time series of intensities.

Introduction

Visual stimuli as encountered by animals in natural scenes are very different from random stimuli. They display strong correlations in space, time and wavelength (van Hateren, 1993; Dong & Atick, 1995), and often encompass a large range of intensities and contrasts. Much of the processing in the early stages of visual processing, in particular those in the retina, is concerned with reducing these correlations and compressing the intensity and contrast ranges such that they fit the limited dynamic range of the retinal neurons. An important goal of visual neuroscience is to understand the mechanisms by which decorrelation and dynamic range reduction are accomplished, and how these influence visual perception.

In this paper we concentrate on the first step in visual processing, as takes place in the vertebrate cone photoreceptors. In particular, we are interested in how natural stimuli are processed, and if the critical physiological steps involved can be identified and understood. We use goldfish cones as our model system, because it is possible to obtain good and stable measurements from these cells. As stimulus we use a natural time series of intensities (NTSI) recorded outdoors. Such NTSIs contain a high dynamic range, a wide temporal frequency bandwidth, and considerable temporal correlations.

Although it is often argued that the early steps in visual processing are essentially linear (see for example Vu *et al.* 1997), we will show here that assuming linearity is not correct for natural stimuli. The high dynamic range of such stimuli causes the cone to display marked non-linearities and a non-linear model seems thus necessary to adequately describe its responses. Analysing the experimental results with the photoreceptor model developed by van Hateren

DOI: 10.1113/jphysiol.2009.179036

and co-workers (2005; van Hateren & Snippe, 2007) shows that the non-linearities can be fully accounted for from what is known on the phototransduction system (Pugh & Lamb, 2000). Membrane non-linearities only contribute slightly. Moreover, we will show that the goldfish cone performs remarkably similar to the cones of primates, including man, only with slower kinetics.

Methods

Preparation

All experimental procedures adhered to the Association for Research in Vision and Ophthalmology (ARVO) Statement for the Use of Animals in Ophthalmic and Vision Research, conformed to the guidelines for the Care and Use of Laboratory Animals of The Netherlands Institute for Neuroscience acting in accordance with the European Communities Council Directive of 24 November 1986 (86/609/EEC) and are in accordance with the policy of *The Journal of Physiology* as outlined by Drummond (2009).

Goldfish, *Carassius auratus* (12–16 cm standard body length), were kept at 18°C under a 12 h dark, 12 h light regime. The fish were kept in the dark for 5 min to facilitate the isolation of the retina from the pigment epithelium while preventing complete dark adaptation, stunned and decapitated in the dark. All further steps in the preparation were performed in the dark under dim red ($\lambda = 650$ nm) illumination. An eye was enucleated, was hemisected and most of the vitreous was removed with filter paper. The retina was isolated and placed, receptor side up, in a recording chamber and superfused continuously (1.5 ml min^{-1}) with oxygenated Ringer solution (pH 7.8, 20°C). For the experiments reported in the paper 27 goldfish were used.

The recording chamber was mounted on a microscope equipped with infrared ($\lambda > 800$ nm; Kodak wratten filter 87c, USA) differential interference contrast optics (model Eclipse E600-FN, Nikon, Japan). The preparation was viewed on an LCD monitor by means of a ×60 water-immersion objective (N.A. 1.0) and a CCD camera (Philips, the Netherlands).

Recordings were made from individual members of double-cones. These cones are either medium- or long-wavelength sensitive (M or L); neutral density filters were used to stimulate both cone types approximately equally strong at the wavelengths used in the experiments. For this paper, the responses of 15 cones were evaluated in detail. Because of limited recording time not all stimulus protocols could be run on all cells, but a subset of the flash stimuli was run on all cells as a reference. All cells responded similarly.

Solutions

The Ringer solution contained (in mM): 102.0 NaCl, 2.6 KCl, 1.0 $MgCl_2$, 1.0 $CaCl_2$, 28.0 $NaHCO_3$, 5.0 glucose and was continuously gassed with 2.5% CO_2 and 97.5% O_2 yielding a pH of 7.8.

The pipette medium contained (in mM): 10 KCl, 96 potassium gluconate, 1 $MgCl_2$, 0.1 $CaCl_2$, 5 EGTA, 5 Hepes, 5 ATP-Na_2, 1 GTP-Na_3, 0.2 3′:5′-cGMP-Na, 20 phosphocreatine-Na_2, 50 units ml^{-1} creatine phosphokinase. The pH of the pipette medium was adjusted to 7.2 with KOH. All chemicals were supplied by Sigma (Zwijndrecht, the Netherlands).

Liquid junction potential

The liquid junction potential was measured with a patch pipette filled with the pipette medium and positioned in a bath filled with the pipette medium. After the potential was adjusted to zero, the bath solution was replaced with Ringer solution. The resulting potential change was considered to be the junction potential and all data were corrected accordingly.

Electrodes and recording equipment

Patch-pipettes were pulled from borosilicate glass capillaries (GC150TF-10, Harvard Apparatus Ltd, UK) with a Brown-Flaming micropipette puller (P-87, Sutter Instruments Company, USA) and had resistances between 5 and 8 MΩ when filled with pipette solution and measured in Ringer solution. Series resistances ranged from 100 to 200 MΩ and were corrected for offline. The electrodes were placed in a PCS-5000 patch clamp micromanipulator (Burleigh Instruments, Inc., USA) and connected to a Dagan 3900A Integrating Patch Clamp amplifier (Dagan Corporation, USA). Data acquisition and control of the optical stimulator were done with a CED 1401 Plus AD/DA converter, Signal software (Cambridge Electronic Design Ltd, UK) and a Windows XP (Microsoft Corporation, USA) -based computer system. Recordings were performed in current-clamp mode, with the holding current kept at 0 pA. Data were sampled at 1 kHz for all stimulus protocols and filtered at 1 kHz using a four-pole Bessel filter.

Optical stimulator

The visual stimulus was generated by a light-emitting diode (LED) with a peak wavelength at 526 nm and a bandwidth of 47 nm (HLMP-CM15-S0000, Agilent Technologies, Inc., USA). The light of the LED was focused onto the retina through the objective of the microscope by means of mirrors and lenses to form

a homogeneous spot with a diameter of 30 μm. The output of the LED at the focal plane was measured with a radiometer (model 50-245, irradiance head J1812, Tektronix, UK). The original stimuli were corrected for measured non-linearities between the light output and the driving voltage. Mean illuminance levels were changed by insertion of neutral density filters (Schott, Germany).

Stimuli

Classical stimuli. Two types of classical stimuli were used, pulses and sinusoids. Flash data were obtained at Weber contrasts, $(I_{max} - I_{min})/I_{min}$, of 2 and 8. Flashes lasted for 10 or 500 ms. For flash stimuli, the highest background light level (I_0 in Fig. 3) corresponded to 9.3×10^4 photons μm^{-2} s^{-1}. Light levels 10 and 100 times lower were obtained by using neutral density filters. Responses to sinusoids were obtained at Michelson contrasts, $(I_{max} - I_{min})/(I_{max} + I_{min})$, of 50% and 100%, and at temporal frequencies of 0.5, 2, 5 and 15 Hz. For sinusoids the mean light level corresponded to 4.8×10^5 photons μm^{-2} s^{-1}.

Natural time series of intensities. A NTSI was used as an appropriate 'natural' stimulus for cones. The NTSI was measured with a light detector worn on a headband by a person walking through a natural environment (van Hateren, 1997; van Hateren & Snippe, 2001). The acceptance angle of the light detector was approximately 2 arcmin, and followed the direction of view of the face (see van Hateren, 1997, for further details). Obviously, an NTSI thus measured is not identical to an intensity series that a goldfish cone would normally encounter: the environment is quite different as well as many parameters, such as speed and behaviour of the organism, average distance to objects, and acceptance angle of the cones. Although it can be argued that several of these parameters cancel each other, and that scale-invariance of the environment will produce NTSIs for different organisms that are not so different (van Hateren, 1997), such arguments are not essential for the present study. The only critical requirement of the stimulus is that the stimulus is sufficiently rich, i.e. that it contains variations in intensity and contrast with a natural mixture of predictability and unpredictability. These variations will presumably drive the cones into regimes of gain control similar to those engaged in truly natural circumstances. For the present experiments we carefully selected a 1 min section of an NTSI that was representative (in power spectrum, dynamic range and temporal structure) of the entire database of NTSIs recorded (12 NTSIs of 45 min each).

For the NTSI stimulus, the mean light level corresponded to 1.5×10^5 photons μm^{-2} s^{-1}. The NTSI was presented at a sample rate of 1 kHz and responses were averaged over five repetitions.

Phototransduction model

Figure 1 shows the phototransduction model used in the present study. It is identical to the one developed in van Hateren (2005) (see also van Hateren & Lamb, 2006) as part of a model that describes responses in macaque H1 horizontal cells. Photocurrent in that model is generated in accordance with the current standard model. Briefly, light (I) excites visual pigment R converting it into R^* (where the latter has a lifetime τ_R). R^* excites a G-protein, G, converting it into G^* which quickly binds with phosphodiesterase (PDE). This activated PDE, E^*, (with a lifetime τ_E) hydrolyses cGMP, and thus causes closing of cyclic nucleotide gated channels which are normally held open by cGMP. The result is that the current entering the cell is reduced, and that the cell

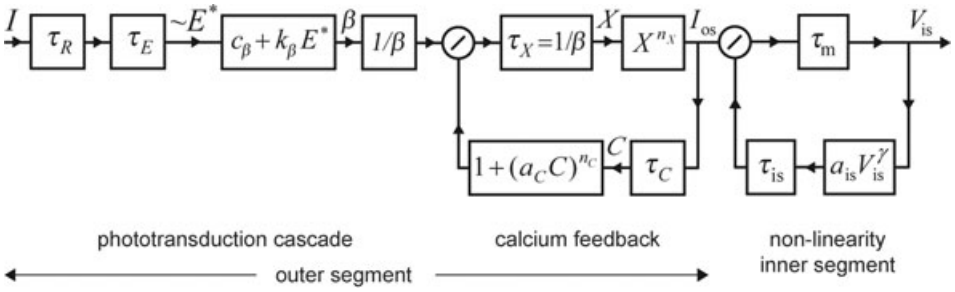

Figure 1. Photoreceptor model
Boxes containing a τ represent first-order low-pass filters of unit DC-gain. Other boxes represent linear or non-linear transformations of variables. Photopigment excited by light (I) has a lifetime τ_R and excites a G-protein that quickly forms a complex E^* (with lifetime τ_E) with phosphodiesterase (PDE). PDE can hydrolyse cGMP at a rate β, which consists of a dark activity c_β by unexcited PDE, and a light-dependent part $k_\beta E^*$. The cGMP concentration (X) opens transduction channels (with apparent cooperativity n_X) producing current I_{os} into the cone's outer segment. Part of the current consists of calcium (C, extruded with a time constant τ_C), which drives cGMP synthesis (with cooperativity n_C) and thus produces a feedback. I_{os} drives the non-linear membrane of the inner segment, with a gain dependent on the membrane potential V_{is}. For more details see van Hateren (2005).

Table 1. Parameters and variables used in the model; see Fig. 1

Symbol	Description	Units	Goldfish value (this study)	Macaque value (van Hateren, 2005)
τ_R	Time constant of R^* inactivation	ms	20 ± 10	3.4
τ_E	Time constant of E^* inactivation	ms	30 ± 16	8.7
c_β	Rate constant of cGMP hydrolysis in darkness	$(\text{ms})^{-1}$	3×10^{-3} (fixed)	2.8×10^{-3}
k_β	Rate constant of cGMP hydrolysis	$(\text{td})^{-1}$	$(2.1 \pm 2.1) \times 10^{-4}$	1.6×10^{-4}
β	cGMP hydrolysis rate	$(\text{ms})^{-1}$	—	—
τ_X	Time constant of cGMP turnover	ms	—	—
X	Scaled cGMP concentration	a.u.	—	—
n_X	Apparent Hill coefficient of CNG activation	—	1 (fixed)	1
I_{os}	Scaled photocurrent of outer segment	a.u.	—	—
τ_C	Time constant of Ca^{2+} extrusion	ms	18 ± 12	3
C	Scaled Ca^{2+} concentration	a.u.	—	—
a_C	Scaling constant of GC activation	a.u.	0.1 (fixed)	9×10^{-2}
n_C	Apparent Hill coefficient of GC activation	—	4 (fixed)	4
α	GC activity	a.u.	—	—
τ_m	Capacitive membrane time constant	ms	15 (fixed)	4
V_{is}	Membrane voltage of inner segment	mV	—	—
γ	Parameter of membrane non-linearity	—	0.85 ± 0.32	0.7
a_{is}	Scaling constant of membrane non-linearity	$(\text{mV})^{-1-\gamma}$	$(4.7 \pm 4.1) \times 10^{-2}$	7×10^{-2}
τ_{is}	Time constant of membrane non-linearity	ms	300 (fixed)	90

Values show mean and standard deviation of parameter values obtained from all model fits made for all individual cones and stimuli. Parameters with fixed values could not be well determined in the fits to the present set of stimuli and were either set close to the macaque value or fitted by hand to yield acceptable fits for the entire set of stimuli and cells. Notes: the smallest of the values at τ_R and τ_E is arbitrarily assigned to τ_R; a.u., arbitrary unit.

hyperpolarizes. Since part of the current is carried by Ca^{2+}, and Ca^{2+} is actively extruded from the cell by a Na–Ca exchanger, the intracellular Ca^{2+} concentration declines as well. This will affect two negative feedback pathways in the cone outer segment. In the first, the efficacy of cGMP binding to the channels is regulated by Ca^{2+}, effectively reducing the apparent Hill coefficient of channel activation to $n_X = 1$ (van Hateren, 2005). In the second, the production of cGMP by guanylyl cyclase is regulated by Ca^{2+}. Ca^{2+} kinetics is determined by the Na–Ca exchanger (producing a time constant τ_C). The photocurrent drives the inner segment of the cone to yield the photovoltage, which is modelled by a non-linear feedback using a scheme presented in Detwiler *et al.* (1980). The phototransduction model is described by the following equations:

$$\mathrm{d}R^*/\mathrm{d}t = (I - R^*)/\tau_R \quad (1)$$

$$\mathrm{d}E^*/\mathrm{d}t = (R^* - E^*)/\tau_E \quad (2)$$

$$\beta = c_\beta - k_\beta E^* \quad (3)$$

$$\mathrm{d}X/\mathrm{d}t = \alpha - \beta X \quad (4)$$

$$\mathrm{d}C/\mathrm{d}t = (I_{os} - C)/\tau_C \quad (5)$$

$$\alpha = 1/[1 + (a_c C)^{n_c}] \quad (6)$$

$$I_{os} = X^{n_x} \quad (7)$$

$$\mathrm{d}V_{is}/\mathrm{d}t = (I_{os}/g_i - V_{is})/\tau_m \quad (8)$$

$$\mathrm{d}g_i/\mathrm{d}t = \left(a_{is} V_{is}^{\gamma} - g_i\right)/\tau_{is} \quad (9)$$

For further explanation see van Hateren (2005) The parameter values obtained in this study are shown in Table 1, as well as the macaque values for comparison.

Coherence methods

The coherence between model prediction and measured response can be used to quantify model performance by comparing this coherence with the expected coherence inferred from measured response repeatability (Haag & Borst, 1998; van Hateren & Snippe, 2001; van Hateren *et al.* 2002). Briefly, the coherence γ^2 between two signals, $s_1(t)$ and $s_2(t)$, is defined as the square of the cross-correlation of their Fourier transforms, $S_1(f)$ and $S_2(f)$, normalized by their power spectra: $\gamma^2 = \langle S_1 S_2^* \rangle \langle S_1^* S_2 \rangle / (\langle |S_1|^2 \rangle \langle |S_2|^2 \rangle)$, where the brackets denote averaging over a suitable partioning of the signals, and the asterisk denotes the complex conjugate. Spectra were calculated by periodogram averaging of 50% overlapping data segments, with each periodogram the discrete Fourier transform of a $\cos^2$-tapered zero-mean data

segment of 1024 ms, extended by zero-padding to 2048 ms. Results were not strongly dependent on segment length. Expected coherence (Haag & Borst, 1998) can be obtained from responses to repeated stimulus presentations as $\gamma^2_{exp} = SNR/(SNR + 1)$, where SNR is the unbiased signal-to-noise ratio $SNR = [(m-1)/m]\,[S/N] - 1/m$, where S and N are raw signal and noise power spectra, respectively, and m is the number of stimulus repeats (van Hateren & Snippe, 2001; van Hateren *et al.* 2002). It is convenient to collapse γ^2 and γ^2_{exp}, which are functions of frequency, into a single number. The most straightforward way to do that is by defining a coherence rate $R_{coh} = -\int_0^\infty \log_2(1-\gamma^2)df$ and an expected coherence rate $R_{exp} = -\int_0^\infty \log_2(1-\gamma^2_{exp})df$ (for discussion of the rationale of these equations see van Hateren & Snippe, 2001). The specific form of these expressions is closely related to Shannon's equation (Shannon, 1948), and coherence rate is therefore expressed in bit s^{-1}. It should be noted, however, that it is a biased estimate (an upper bound) of the information rate because not all signals involved are Gaussian (van Hateren & Snippe, 2001). To avoid confusion, we will therefore use the term 'coherence rate' rather than 'information rate'.

Results

Van Hateren (2005) formulated a model for vertebrate photoreceptors based on known physiological processes of the phototransduction cascade. The model is highly non-linear and forms the basis for an outer retinal model describing the responses of horizontal cells in primate retina. The model was successfully used to evaluate human electroretinogram (ERG) data (van Hateren & Lamb, 2006). So far the photoreceptor part of the model was not tested directly on photoreceptor responses. Validating that model is a major aim of the present study because it provides insight into which dynamical processes in the cone determine its response characteristics. In order to estimate the parameters of the photoreceptor model, we studied the dynamic properties of light responses of goldfish L- and M-cones to short and long flashes of light and sinusoidally modulated light and compared these responses to the responses of the model photoreceptors when stimulated with the same stimuli as used during experiments.

As the pigment epithelium was removed from the retinal preparation used in this study, light intensity levels were chosen such that a negligible fraction of the cone pigment became bleached, because recovery from bleaching may have been reduced or absent in our recording conditions. Furthermore, we used contrasts and light intensities that did not saturate cone responses. To reduce the possible influences of negative feedback from horizontal cells to cones on the responses, we used a small spot of light with a diameter of 30 μm to limit horizontal cell polarization. Moreover, it has previously been shown that under our experimental conditions ($E_{Cl} = -55$ mV) surround stimulation does not lead to polarization of cones (Kraaij *et al.* 2000).

Responses to flashes

The responses of cones to flashes of either 10 or 500 ms at a Weber contrast of either 2 or 8 at three different light levels were studied first. The first three panels of Fig. 2 show the responses to flashes of 500 ms with contrasts of 2 and 8 together with the responses of the cone model. The three light levels are indicated at the top of the panels. Note that the scaling of the voltage axis is different for each panel.

The cone responses to 500 ms flashes are relatively sustained with a sag-back after light onset and response overshoot at light offset for all intensities and contrasts. For equal contrasts, response amplitudes increase with light level, i.e. goldfish cones do not respond according to Weber's law at these intensities. At each intensity level a non-linear relationship was found between flash contrast and response amplitude: the response amplitude to the flash with a Weber contrast of 8 was always smaller than 4 times the response amplitude to the flash with a Weber contrast of 2.

Figure 2*D* displays the responses to 10 ms flashes at the highest light level. The responses are slightly biphasic and the response amplitude at Weber contrast 8 is smaller than 4 times the response amplitude at Weber contrast 2. Since the duration of the 10 ms flash stimulus is considerably shorter than the integration time of the cone, the responses do not reach the same amplitude as with 500 ms flashes of corresponding contrasts.

The red continuous lines in Fig. 2 are responses of the model cones. These curves were simultaneously fitted to the complete data set for each cell. Comparison of the red curves and the actually measured responses shows that they both have the same response characteristics. See Discussion for detailed interpretation.

Reponses to sinusoids

Next, light responses to sinusoidal modulation were measured at frequencies of 0.5, 2, 5 and 15 Hz and Michelson contrasts of 50% and 100%. Figure 3 shows an example of the responses of an L-cone together with the responses of the cone model to the same stimuli. The different panels show the responses to different stimulation frequencies as indicated in each panel. The scaling of the time axis is chosen such that for each frequency the response to two stimulus periods is shown. The stimuli are displayed at the bottom of the figure.

Goldfish cones are capable of following the sinusoidal stimulus at the highest temporal frequency used i.e. 15 Hz (Fig. 3*D*). Beyond 2 Hz stimulation (Fig. 3*B*), increased temporal frequencies yield decreased response amplitudes (Fig. 3*C* and *D*). At low and intermediate frequencies two different distortions are present, especially at high contrasts. At low frequencies (Fig. 3*A*), the distortion consists of an asymmetry around the response level produced by the mean intensity (dashed line). The result is a flattening of the hyperpolarization to the maximum of the stimulus and a sharpened shape of the depolarization to the minimum of the stimulus. At intermediate frequencies (Fig. 3*B* and *C*), an additional distortion, consisting of an asymmetry around the vertical axis, gives the response a sawtooth-like appearance. The hyperpolarizing flank has become faster than the depolarizing flank of the response to the sinusoid.

Next the photoreceptor model was fitted to the voltage responses. The red lines in Fig. 3 show the simulated responses. They were simultaneously fitted to the complete data set for each cell. The model fits adequately describe all the characteristics of the real cone responses (see the Discussion for a detailed interpretation).

To check whether these non-linearities were due to membrane properties or due to properties of the phototransduction cascade, we recorded the responses of cones when they were voltage clamped at −80 mV and stimulated by a 8 Weber 500 ms flash or a 2 Hz 100% contrast sinusoid. Figure 4 shows that the non-linearities found in the voltage responses were also present in the current responses. The sag-back and the overshoot are both present in the current response but seem to be much smaller compared to the voltage response. This indicates that the sag-back and off-overshoot are partly due to the non-linear behaviour of the membrane. The current responses to the sinusoids show both non-linear features, the flattening of the response and the sawtooth-like behaviour. They are equal in strength in both the voltage and the current responses. This shows that the non-linear behaviour is due to non-linear properties of the phototransduction cascade.

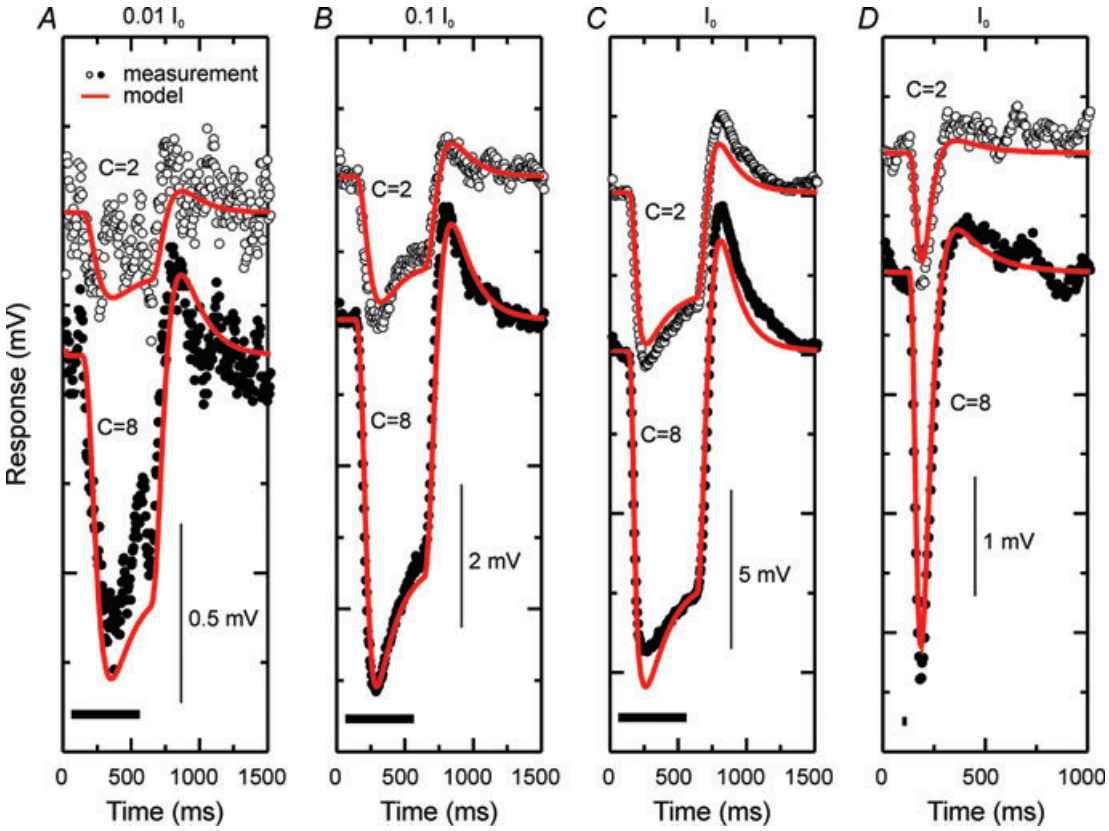

Figure 2. Responses of a cone photoreceptor and the phototransduction model to flashes
The four panels show the responses of a cone (dots) and the phototransduction model (red lines) to light flashes at three different light levels as indicated above the panels with 1 log unit steps. Flashes were of a Weber contrast of 2 (open dots and red line) or 8 (filled dots and red line), which is indicated near the traces in the panels. The stimulation period is marked by the thick black line below the responses. For *A*–*C* the flash lasted 500 ms. The stimulus of *D* had a duration of 10 ms and was performed at the same light level as *C*. For all panels the voltage axis has different scaling as indicated within each panel. The same parameter values are used for all model responses.

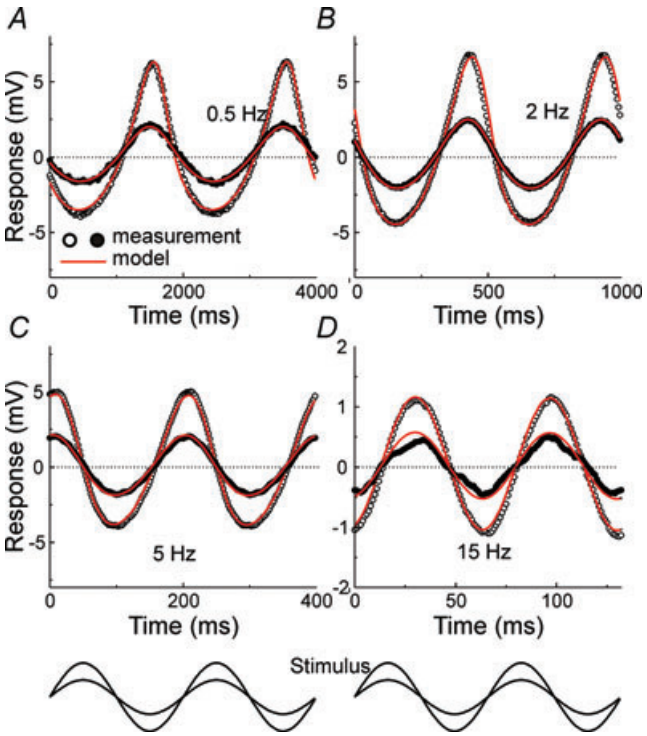

Figure 3. Responses of a cone photoreceptor and the phototransduction model to sinusoids
The panels show the voltage responses of a cone (dots) and the photoreceptor model (red line) to sinusoidal light stimulation of four different frequencies as indicated within each panel. Shown are the responses for two periods of stimulation, which are illustrated below the panels. For these responses, stimuli had a Michelson contrast of 50% (filled dots) and 100% (open dots). Note the different *y*-axis scaling for each stimulation frequency. The dashed line is the response level produced by the mean light intensity. The same parameter values are used for all model responses. Recordings are from a different cone than in Fig. 2.

Cone responses to a natural time series of intensities

To investigate the processing strategy of goldfish cones under natural stimulus conditions, we recorded their responses to a NTSI. The NTSI is plotted as a function of time in Fig. 5*A*. The time series shows a low mean intensity with occasional high intensity peaks. The probability density function (pdf), which is displayed to the right of the time series, shows the relative occurrence of each intensity level. The time series shows a distribution which is skewed towards the lower intensities and has a long tail into the higher intensity region. This kind of pdf is typical of NTSIs (van der Schaaf & van Hateren, 1996; Burkhardt *et al.* 2006).

The NTSI was reproduced on an LED, and projected onto the cones at a light intensity avoiding significant pigment bleaching. A typical response of a cone stimulated with the NTSI is shown in Fig. 5*B* (left). The pdf of the response (Fig. 5*B*, right) is transformed compared to that of the original stimulus (Fig. 5*A*, right). Unlike the pdf of the stimulus, the pdf of the response is more symmetrical in shape. The pdf of the response shows that the cone devotes a large proportion of its dynamic range to the NTSI's lower intensities.

Model responses to a natural time series of intensities

Figure 5*C* shows the response of the photoreceptor model to the NTSI with parameters fitted for this cell. Comparing Fig. 5*B* and *C* indicates that the model captures most of the details of the cone response. The pdf of the model responses is similar to that of the cone. Next we evaluated whether a linear filter yields a similar good performance. This filter is the optimal linear filter as provided by the coherence analysis of stimulus and response. Although a linear filter (Fig. 5*D*) captures the large intensity changes adequately, it under-represents the responses to low intensities. For instance, the small intensity changes in the two enlarged sections shown in Fig. 5*E* and *F* are well represented by both the real cone and the photoreceptor model. They are much smaller in the response of the linear filter (Fig. 5*D* and *E*). At the right-side of Fig. 5*D* the pdf of the responses for the linear filter is given. Like the photoreceptor model and the cone response, it

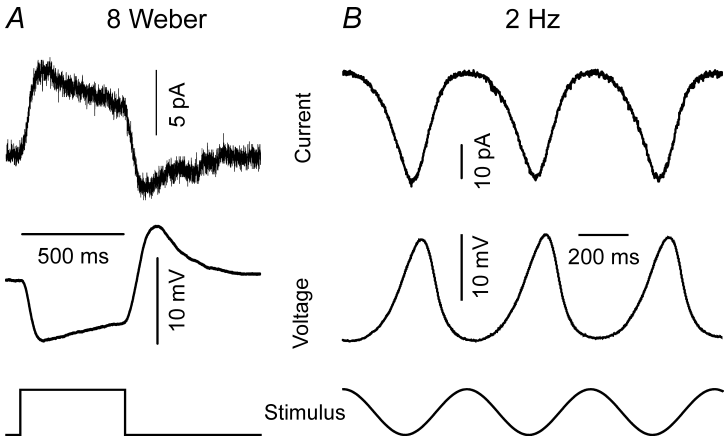

Figure 4. Voltage and current responses of a cone photoreceptor
A, current (top) and voltage (bottom) responses of a cone when stimulated with a 500 ms flash of 8 Weber. Both responses show a biphasic nature. However, the biphasic nature in the voltage response is much stronger than for the current response. *B*, current (top) and voltage (bottom) responses of a cone when stimulated with a 2 Hz 100% contrast sinusoid. The 'flattening' and the 'sawtooth' non-linearities are visible in both traces to the same extent, indicating that these two non-linearities originate in the phototransduction cascade.

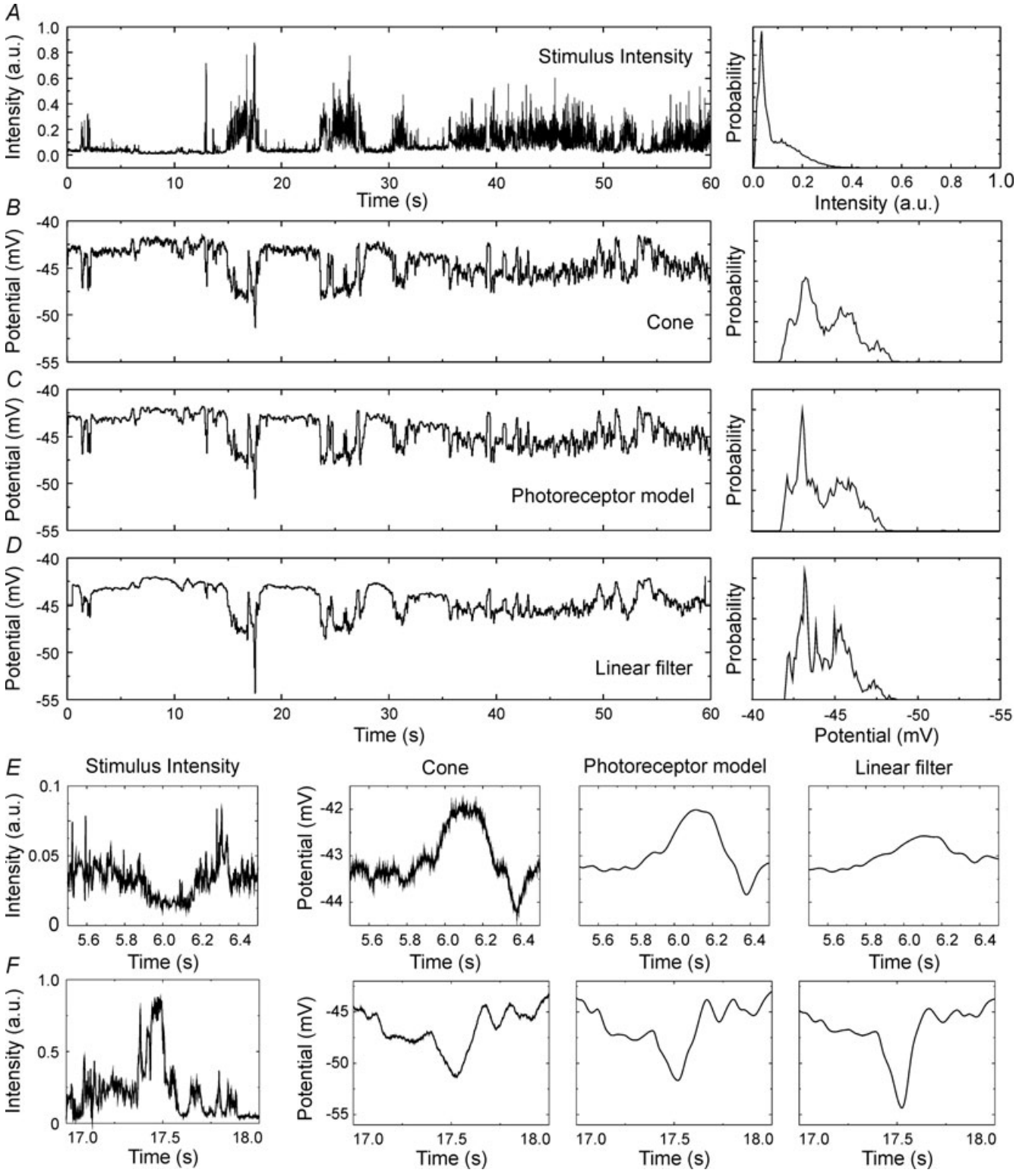

Figure 5. Responses of a cone photoreceptor and different models to a natural time series of intensities
A, the recorded natural time series of intensities (NTSI). On the right side of this panel, its corresponding probability density function (pdf) is plotted. *B*, the response (average of 5 individual responses) and resulting pdf of a cone photoreceptor where the NTSI was used as stimulus. *C*, the response and pdf of the phototransduction model when fitted to the cone of *B*. *D*, the response and pdf to the NTSI when using the linear filter that optimally transforms the stimulus into the measured response. *E*, detailed view of stimulus and responses around time = 6.0 s. *F*, detailed view of stimulus and responses around time = 17.5 s. Recordings are from a different cone than in Figs 2 and 3.

yields a distribution which is much more compact than that of the stimulus. It lacks the long tail present in the stimulus at high intensities because the sparse high intensity peaks are suppressed. As a result the dynamic range of the response is reduced. Whereas this compression of the dynamic range is partly attributable to non-linearities in the photoreceptor model, for the linear filter it is attributable purely to low-pass filtering. Since high intensity peaks are sparse and therefore tend to be short in duration, they are particularly reduced by low-pass filtering.

Finally, we quantified the performance of the photoreceptor model and the optimal linear filter using two parameters: i.e. the coherence and the coherence rate. The amount of coherence tells us, as a function of frequency, what fraction of the measured response is linearly related to the computed response (see Methods for a mathematical description). Roughly speaking it is like the squared correlation coefficient at each frequency component. The coherence is calculated between the noise-free model response and the measured individual response traces, and therefore is ultimately limited by the signal-to-noise ratio of the cone. For the measured cone responses a coherence (expected coherence) can be obtained from the response repeatability (see Methods). It can be interpreted as the coherence between the true mean of the response (which would have been obtained from averaging an infinite number of response traces) and the individual response traces. It is therefore the maximum coherence any model predicting the mean response could yield. The coherences of the photoreceptor model, the linear filter, and the cone (expected coherence) are plotted in Fig. 6. The phototransduction model has a coherence which is close to that of the cone itself; the linear filter performs less well. The amplitude transfer function, the inset in Fig. 6, shows that the linear filter is essentially a low-pass filter.

Integration of the coherence over the frequency range yields the coherence rate (R_{coh}, see Methods for a mathematical description). It is expressed in bit per second because it is related to the information rate. The coherence rate of the cone itself (R_{exp}) is the maximum that can be attained by any model. The average coherence rate of cones measured was 43 ± 6 bit s^{-1} ($n = 11$) and is set to 100%. The linear filter captures 48 ± 8% of the coherence rate of the cone, compared to 91 ± 5% by the phototransduction model as fitted to each individual cone. The phototransduction model with a generic parameter set (Table 1, average parameter values obtained from all fits to all cones) still yields 87 ± 8% of the cone coherence rate.

Discussion

In this paper we examined the response behaviour of cones to a NTSI. We found that a strong response compression occurs already in the cones. Low light intensities receive a higher gain than high intensities. Consequently, the skewed intensity distribution found in NTSIs is transformed into a more symmetrical distribution of cone responses, in which small contrast modulations are well represented. It is this distribution which is ultimately transmitted to higher-order neurons. We evaluated two approaches to describe this behaviour of the cones: an optimal linear filter and a non-linear model incorporating known features of the phototransduction. Although the compressive transformation of the light distribution occurs in both approaches, the cone responses to small contrast modulations are best reproduced by the non-linear model. These results indicate that cones perform a non-linear transformation on a NTSI.

The photoreceptor model (van Hateren, 2005) used here is based on known processes of the phototransduction of cones and is highly non-linear. It was used in a model of the primate outer retina to evaluate horizontal responses and to evaluate human ERG responses. The present study is the first study in which the model is directly compared to responses of cones themselves and shows that the photoreceptor model adequately describes the properties of cones for classical and natural stimuli. It describes the cone responses significantly better than a linear filter.

The responses measured in goldfish cones are qualitatively very similar to the corresponding measurements on macaque horizontal cells presented by Smith *et al.* (2001). Nearly the same distortions in response to sinusoids are observed, as well as a similar non-linear contrast–response relationship and a similar

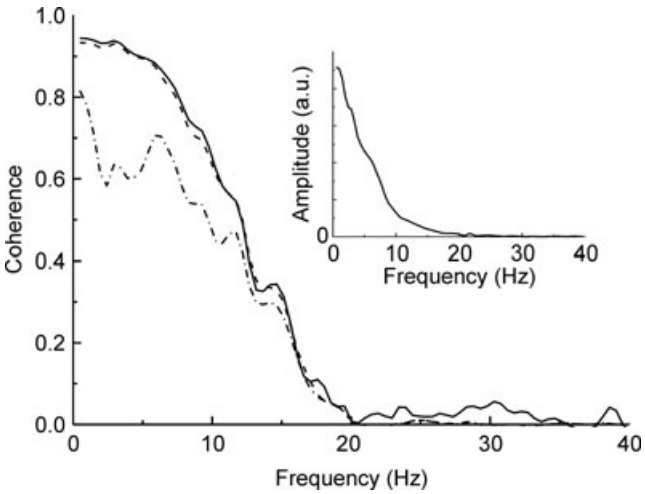

Figure 6. Coherence of a cone photoreceptor and different models
The coherences calculated for the same cone photoreceptor as in Fig. 3 (continuous line, expected coherence), the photoreceptor model (dashed line), and the optimal linear filter (dash–dot line) over the frequency range. The inset displays the amplitude transfer function of the linear filter.

change in gain as a function of background light level. From the model fits performed here and in van Hateren (2005) we can quantitatively compare the properties of primate and goldfish cones. Evaluation of the parameter sets used to describe the goldfish and the primate cones shows that they are remarkably similar (Table 1). The major difference between the two sets of parameters is that the time constants for the macaque cones are shorter, showing that primate cones are faster than goldfish cones. The possible reason for this difference in time constants might be the temperature of the preparation during the experiments. The responses of goldfish cones were recorded at room temperature (20°C) whereas the responses of macaque horizontal cells were recorded at 36°C (Dacey & Lee, 1994). Given a Q_{10} between 2 and 4 (Schellart *et al.* 1974), this temperature difference can account for the differences in time constants. The close correspondence of the other parameters between the goldfish and macaque cones may reflect the high level of conservation in the phototransduction machinery between these species.

Responses to light flashes

To assess the dynamic properties of cones we have used flashes of light upon different background light levels. For these flashes we used Weber contrasts; this implies that the absolute intensity of the flash increases with increasing background intensities. We find that this kind of stimulation results in increasing response amplitude for the same contrast when increasing background intensities. Therefore, for the light levels we used, cones did not show contrast constancy, i.e. did not follow Weber's law. Burkhardt (1994) found similar results in turtle cone photoreceptors and showed that increasing light levels even further leads to a stabilization of the response amplitude for the same contrast. In that case, cones do show contrast constancy. Likewise, macaque horizontal cells display increasing response amplitudes for increased background intensities (Smith *et al.* 2001). As a remark we note that many researchers use constant flash amplitudes for different background light levels. This causes the Weber contrast to decrease with increasing light levels resulting in lowering of the response amplitude. It should be stressed that this is fully consistent with our present results.

The pulse responses shown in Figs 3 and 4 are biphasic. The biphasic character is less present in the current responses compared to the voltage responses showing that a large part of the biphasic nature of the response is due to non-linear membrane properties of the cone, but that a small contribution of the phototransduction cascade cannot be excluded. Soo *et al.* (2008) also showed a biphasic character of the current response. In literature it has been reported that cone current responses to short flashes are monophasic (Dunn *et al.* 2007, their Fig. 1e). Also, cone current responses derived from short flash ERG measurements on human retina show monophasic characteristics (van Hateren & Lamb 2006). These authors argued that the biphasic nature of the voltage response is fully dependent on non-linear membrane properties. This suggests that the membrane non-linearities are dominating in the short flash responses and that at longer stimulus durations the non-linearity of the phototransduction cascade starts to contribute.

The origin of sine-wave distortions in cone responses

The responses of goldfish cones display two characteristic distortions to sinusoids: asymmetric responses around the mean level at low frequencies and a sawtooth-like distortion at intermediate frequencies. These become more apparent at higher contrasts. Such distortions are also found in the macaque H1 horizontal cell (Smith *et al.* 2001) and are indicative for processing non-linearities. Very similar distortions were found in cat horizontal cells as well (Lankheet *et al.* 1991). Detailed modelling (van Hateren, 2005) suggested that the origin of these non-linearities can be found in the phototransduction cascade in cones. Although we did not test the involvement of the various components of the phototransduction cascade directly, the excellent fit between the experimental data and the model behaviour over a wide range of stimulus conditions, provides strong support for this suggestion.

In the model of van Hateren the activity of PDE is defined as β. As discussed in van Hateren (2005) $1/\beta$ turns out to be a very important value for setting the sensitivity and the time constant of the system. The first distortion, which is the asymmetry around the resting level, is mainly produced by this static non-linearity $1/\beta$. The low intensity part of the sinusoidal stimulus leads to a small β and successively a large $1/\beta$ and thus a large response. In the high intensity part of the sinusoid, β is large and in that way reduces the response amplitude. The calcium-feedback loop will also contribute to this distortion, although to a lesser extent. The second distortion, the sawtooth-like distortion with the falling flank steeper than the rising flank, originates from the low-pass filter properties of the calcium-feedback loop. When the light intensity starts to rise from the trough of the sinusoid, β is small but gets larger and therefore $1/\beta$ gets smaller quickly. Normally this would be moderated by the negative feedback of the calcium loop, but because β is still small at this point in time the associated time constant $\tau_X = 1/\beta$ is long and it therefore takes some time before the calcium feedback becomes effective. Therefore the falling flank of the response is steep. At the rising flank, β changes from large to small, therefore τ_X is short and the calcium feedback acts quickly to make the flank less steep than it would have been without calcium feedback.

van Hateren (2005) describes a third kind of distortion to sinusoids in macaque horizontal cells responses, which can also be found in cat horizontal cells. This distortion occurs at high frequencies (about 30 Hz) and leads to a steeper depolarizing flank compared to the hyperpolarizing flank. This distortion was suggested to be due to negative feedback from horizontal cells to cones which only affects the horizontal cell membrane potential and not the cone membrane potential (van Hateren, 2005). This is consistent with physiological results from Kraaij *et al.* (2000). Moreover, possible feedback responses that would be visible in the cones have been strongly reduced by our experimental approach (see beginning of Results). Consistent with this approach and the hypothesis that the third type of distortion is generated by the horizontal cells, we did not find any evidence for this type of distortion in our cone data.

Functional role of cone non-linearities

A major function of cones is to ensure that the very wide range of intensities and contrasts encountered in natural environments is compressed in such a way that the signals fit into the cell's response range. The major strategy to accomplish this used by vertebrate cones is the hydrolysis of cGMP by activated PDE, a non-linear process that causes an inverse relationship between light intensity and channel opening ($1/\beta$). The dynamics of the non-linear equation governing this process are such that it also makes the cone faster at higher background intensities. However, the inverse relationship does the job too well: it would over-compress natural intensities, leading to a skewed distribution once more, but now with a long tail not at high intensities but at low intensities (see the Supplementary Material of van Hateren (2005) for a mathematical analysis, and van Hateren & Snippe (2006) for a graphical illustration). The calcium-feedback loop reduces the effect of the $1/\beta$ non-linearity through negative feedback, bringing the transformation closer to what is required for natural intensity distributions. Similarly, the dynamic non-linearity of the inner segment (essentially a band-pass filter) helps to further reduce the required response range. In Fig. 3 of van Hateren & Snippe (2007) the relative contribution of the various processes can be seen. Eventually, all processes in the cone contribute towards reaching contrast constancy (i.e. the same response to a given contrast independent of background light level) in the visual system.

Linear or non-linear processing in photoreceptors

The processing strategy of cone photoreceptors was tested experimentally by stimulation with a NTSI. These stimuli show a large dynamic range with a distribution which is skewed towards the lower intensities or contrasts. We find that goldfish cones when presented with this NTSI partly correct this skewed distribution in their voltage response, whilst enhancing small contrast modulations. The behaviour of cones in our experiments can be best modelled by a non-linear biophysical model. It has been argued that static responses can be described by a logarithmic transformation (Normann & Werblin, 1974; Laughlin & Hardie, 1978; Normann & Perlman, 1979; Laughlin, 1981; see also van Hateren & Snippe, 2006). Such a transformation has an interesting functional interpretation because it implies contrast constancy. We tested a logarithmic transformation of the NTSI for computing the dynamic responses of the present study, i.e. a logarithm followed by the optimal linear filter produced by the subsequent coherence analysis. We found that such a transformation indeed performs significantly better ($65 \pm 6\%$ of the cone coherence rate) than only a linear filter (48%), but also considerably worse than the biophysical photoreceptor model (87–91%). A type of model that has recently gained popularity (e.g. Mante *et al.* 2005) consists of a linear filter followed by a static non-linearity. It is likely that such a model performs at least as good as a logarithmic transformation on the NTSI responses. However, we have not investigated such a model here, because it cannot explain all non-linearities we found (such as the asymmetrical distortion of sinusoids), does not produce changes in speed as a function of background light level (van Hateren, 2005), and has no clear functional or biophysical interpretation.

Vu *et al.* (1997) reported that rod photoreceptors of the salamander behave as linear transducers, using fairly low contrast stimuli obtained from natural environments. Apart from possible differences between rods and cones, we believe that a main reason for the difference between their and our results lies in the contrasts used. Indeed, for low contrasts photoreceptors act as linear transducers in good approximation. Similar results are reported for salamander cones by Burkhardt *et al.* (2006), who show that the contrast–response curve of cones is much shallower than that of bipolar cells for naturally occurring contrasts. However, when one also includes higher contrasts it becomes clear that the photoreceptor actually is a non-linear transducer, which only responds linearly over a limited range of contrasts. This is evident when stimulating with the natural time series of intensities, which contains both low and high contrasts.

Conclusion

The visual system is faced with the task to code the wide range of intensities and contrasts as encountered in natural scenes into a limited neuronal response range. This study directly shows that in goldfish cones much of

the essential compression already takes place in the photoreceptors and can be related to properties of the phototransduction cascade as was suggested by van Hateren (2005) for macaque cones.

References

Burkhardt DA (1994). Light adaptation and photopigment bleaching in cone photoreceptors in situ in the retina of the turtle. *J Neurosci* **14**, 1091–1105.

Burkhardt DA, Fahey PK & Sikora MA (2006). Natural images and contrast encoding in bipolar cells in the retina of the land- and aquatic-phase tiger salamander. *Vis Neurosci* **23**, 35–47.

Dacey DM & Lee BB (1994). The 'blue-on' opponent pathway in primate retina originates from a distinct bistratified ganglion cell type. *Nature* **367**, 731–735.

Detwiler PB, Hodgkin AL & McNaughton PA (1980). Temporal and spatial characteristics of the voltage response of rods in the retina of the snapping turtle. *J Physiol* **300**, 213–230.

Dong D & Atick J (1995). Statistics of natural time-varying images. *Network: Computation in Neural Systems* **6**, 345–358. Informa Healthcare.

Drummond GB (2009). Reporting ethical matters in *The Journal of Physiology*: standards and advice. *J Physiol* **587**, 713–719.

Dunn FA, Lankheet MJ & Rieke F (2007). Light adaptation in cone vision involves switching between receptor and post-receptor sites. *Nature* **449**, 603–606.

Haag J & Borst A (1998). Active membrane properties and signal encoding in graded potential neurons. *J Neurosci* **18**, 7972–7986.

Kraaij DA, Spekreijse H & Kamermans M (2000). The nature of surround induced depolarizing responses in goldfish cones. *J Gen Physiol* **115**, 1–14.

Lankheet MJM, Van Wezel RJA & Van de Grind WA (1991). Effects of background illumination on cat horizontal cell responses. *Vision Res* **31**, 919–932.

Laughlin SB (1981). A simple coding procedure enhances a neuron's information capacity. *Z Naturforsch C* **36**, 910–912.

Laughlin SB & Hardie RC (1978). Common strategies for light adaptation in the peripheral visual systems of fly and dragonfly. *J Comp Physiol A Neuroethol Sens Neural Behav Physiol* **128**, 319–340.

Mante V, Frazor RA, Bonin V, Geisler WS & Carandini M (2005). Independence of luminance and contrast in natural scenes and in the early visual system. *Nat Neurosci* **8**, 1690–1697.

Normann RA & Perlman I (1979). The effect of background illumination on the photoresponses of red and green cones. *J Physiol* **286**, 491–507.

Normann RA & Werblin FS (1974). Control of retinal sensitivity. I. Light and dark adaptation of vertebrate rods and cones. *J Gen Physiol* **63**, 37–61.

Pugh EN & Lamb TD (2000). Phototransduction in vertebrate rods and cones: molecular mechanisms of amplification, recovery and light adaptation. In *Handbook of Biological Physics*, eds. Stavinga DG, De Grip WJ & Pugh EN, pp. 183–254. Elsevier, Amsterdam.

Schellart NAM, Spekreijse H & Van Den Berg TJTP (1974). Influence of temperature on retinal ganglion cell response and ERG of goldfish. *J Physiol* **238**, 251–267.

Shannon CE (1948). A mathematical theory of communication. *Bell System Tech J* **27**, 379–423.

Smith VC, Pokorny J, Lee BB & Dacey DM (2001). Primate horizontal cell dynamics: an analysis of sensitivity regulation in the outer retina. *J Neurophysiol* **85**, 545–558.

Soo FS, Detwiler PB & Rieke F (2008). Light adaptation in salamander L-cone photoreceptors. *J Neurosci* **28**, 1331–1342.

Van Der Schaaf A & van Hateren JH (1996). Modelling the power spectra of natural images: statistics and information. *Vision Res* **36**, 2759–2770.

van Hateren H (2005). A cellular and molecular model of response kinetics and adaptation in primate cones and horizontal cells. *J Vis* **5**, 331–347.

van Hateren JH (1993). Spatial, temporal and spectral pre-processing for colour vision. *Proc Biol Sci* **251**, 61–68.

van Hateren JH (1997). Processing of natural time series of intensities by the visual system of the blowfly. *Vision Res* **37**, 3407–3416.

van Hateren JH & Lamb TD (2006). The photocurrent response of human cones is fast and monophasic. *BMC Neurosci* **7**, 34.

van Hateren JH, Ruttiger L, Sun H & Lee BB (2002). Processing of natural temporal stimuli by macaque retinal ganglion cells. *J Neurosci* **22**, 9945–9960.

van Hateren JH & Snippe HP (2001). Information theoretical evaluation of parametric models of gain control in blowfly photoreceptor cells. *Vision Res* **41**, 1851–1865.

van Hateren JH & Snippe HP (2006). Phototransduction in primate cones and blowfly photoreceptors: different mechanisms, different algorithms, similar response. *J Comp Physiol A Neuroethol Sens Neural Behav Physiol* **192**, 187–197.

van Hateren JH & Snippe HP (2007). Simulating human cones from mid-mesopic up to high-photopic luminances. *J Vis* **7**, 1.

Vu TQ, McCarthy ST & Owen WG (1997). Linear transduction of natural stimuli by dark-adapted and light- adapted rods of the salamander, *Ambystoma tigrinum*. *J Physiol* **505**, 193–204.

Acknowledgements

Both authors were involved in (1) conception, design, analysis and interpretation of the data, (2) drafting the article and (3) final approval of the version to be published. We would like to thank Dr Hans van Hateren for his valuable contributions to the paper. D.E. and M.K. were supported by a grant from ALW-FOM-NWO. This research was supported by European Commission FP7 Grant RETICIRC HEALTH-F2-2009-223156.